Non-coding RNA Research 8 (2023) 579–588

Contents lists available at ScienceDirect

Non-coding RNA Research

journal homepage: www.keaipublishing.com/en/journals/non-coding-rna-research

Original Research Article

miR-346 regulates the development of ARDS by regulating the function of pulmonary microvascular endothelial cells

Jing Jiang [a,1], Fei Guo [b,1], Wei Li [a,*], Xiaoxi Shan [a,**]

[a] Department of Pulmonary and Critical Care Medicine, The Affiliated Yantai Yuhuangding Hospital of Qingdao University, Yantai, Shandong, 264000, China
[b] Department of Pulmonary and Critical Care Medicine, Yantai affiliated Hospital of Binzhou Medical University, Yantai, Shandong, 264100, China

ARTICLE INFO

Keywords:
Apoptosis
ARDS
Mechanism
miR-346
Proliferation

ABSTRACT

In recent years, many studies have reported that microRNAs play an important role in the pathogenesis of a variety of diseases, and the aim of this paper is to explore the role and mechanism of miR-346 in acute respiratory distress syndrome (ARDS). A mouse model of ARDS was constructed by LPS induction, and RT-qPCR assay was used to verify that the expression level of miR-346 in lung tissue was significantly increased, and was negatively correlated with oxygenation index. Inhibiting the expression of miR-346 in mice and HPMECs by miR-346 inhibitor confirmed that decreased miR-346 expression could lead to increased oxygenation index, decreased lung index, lung water content and NO content to reduce lung injury in mice, while lung inflammation was alleviated and apoptosis was reduced in mice. The same results were obtained in cells. BCL6 was predicted to be a target of miR-346 by targetscan and miRDB; when miR-346 was inhibited, BCL6 expression was increased, and if miR-346 and BCL6 expression were inhibited at the same time, it could aggravate lung injury and reduce the proliferation of HPMECs and increase their apoptosis and inflammation in mice. This shows that miR-346 inhibits the migration of HPMECs by regulating BCL6 expression, which in turn promotes the apoptosis of HPMECs, leading to inflammation and inducing ARDS.

1. Introduction

Acute respiratory distress syndrome (ARDS) is an acute hypoxemic respiratory failure syndrome, mainly an inflammatory change of acute diffuse lung injury, resulting in increased pulmonary vascular permeability and increased pulmonary endothelial and epithelial cell permeability [1]. Direct or indirect factors such as lung infection and sepsis can contribute to ARDS [2]. The treatment of ARDS is also evolving, such as mechanical ventilation therapy [3], stem cell therapy [1], and drug therapy [4]. Because of its high morbidity and mortality (10%–90%) [5], which poses a serious threat to patients [6], exploring the pathogenesis and treatment of ARDS is a key issue to be solved urgently at present. Pulmonary capillary endothelial cell dysfunction leads to endothelial cell barrier disruption, a marker of ARDS, and is also one of the causes of clinical protein-rich pulmonary edema. The apoptosis of lung endothelial cells is widespread in ARDS patients [7]. It was previously demonstrated that microvascular endothelial cells promote angiogenesis through a paracrine mechanism [8], whereas in pulmonary microvascular endothelial cells, LPS can increase neovascularization in Matrigel [9].

MicroRNAs (miRNAs) are a class of single-stranded non-coding RNA molecules mainly involved in gene regulation at the post-transcriptional level, which play an important role in the regulation of cell growth and development, immunity and inflammation. Aberrant expression of miR-346 is associated with related diseases such as cervical cancer [10] and osteogenic differentiation [11]. MiR-346 has recently been shown to be associated with inflammatory diseases, such as miR-346 overexpression can reduce myocardial injury and reduce the infarct size by inhibiting myocardial apoptosis [12], suggesting that miR-346 plays an important role in inflammatory signal transduction. In recent years, many studies have shown that microRNAs are involved in ARDS, such as down-regulation of miR-34a expression is able to reduce LPS-induced acute lung injury [13]. miR-155-5p is able to promote the progression of ARDS by inhibiting the expression levels of proteins in the WNT signaling pathway [14]. It has also been shown that miR-346-3p is able to participate in programmed cell necrosis and infection by regulating

* Corresponding author.
** Corresponding author.
E-mail addresses: liw_yuhuangd@sina.com (W. Li), XiaoxiS@tom.com (X. Shan).
[1] These authors contributed equally to this work.

https://doi.org/10.1016/j.ncrna.2023.08.006
Received 3 May 2023; Received in revised form 8 August 2023; Accepted 16 August 2023
Available online 18 August 2023

RIPK1, which in turn leads to tuberculosis [15]. Although bioinformatics has shown that miR-346 expression is upregulated and targets multiple mRNAs in rat ARDS [16], current studies on the mechanism of action of miR-346 in ARDS remain rarely reported.

In this study, ARDS models were constructed by LPS-induced mice to observe the effects of lung sections and miR-346 on the inflammatory and apoptotic responses of ARDS, in order to explore the regulatory mechanism of miR-346 on ARDS and provide new insights and references for the prevention and treatment of ARDS.

2. Materials and methods

2.1. Animal experiments

Sixty mice were provided by Jinan Pengyue Laboratory Animal Co., Ltd (China). All animal experimental procedures were performed according to the guidelines of the National Institutes of Health and approved by the Ethics Committee of Yantai Yuhuangding Hospital (2023-299). After 3 days of regulated feeding, LPS induction or transfection with miR-346 inhibitor and si-BCL6 was performed. A mouse model of acute lung injury was established by intratracheal instillation of LPS (10 mg/kg) (Beijing Solarbio Science & Technology Co., Ltd., Beijing). Healthy control mice received the same amount of saline. miR-346 inhibitor and si-BCL6 were injected into mice according to Entranster™-*in vivo* (Engreen Biosystem, Ltd., China) instructions. One day after injection, mice were stimulated by LPS. One day after LPS stimulation, mice were euthanized and lung tissue, blood, and bronchoalveolar lavage fluid were collected.

2.2. RNA extraction and real-time fluorescence quantification

Lung tissues stored at −80 °C were taken. According to the instructions, total RNA was extracted from the samples using RNAprep Pure Tissue Kit (TIANGEN Biotech Co., Ltd, Beijing, China), and single-stranded DNA was obtained by reverse transcription using HiScript III 1st Strand cDNA Synthesis Kit (+gDNA wiper) (Vazyme Biotech Co., Ltd, Nanjing, China). For miRNA determination, total miRNA was extracted from the samples using miRcute miRNA Isolation Kit (TIANGEN Biotech Co., Ltd, Beijing, China), and first-strand synthesis was performed by HiScript III 1st Strand cDNA Synthesis Kit (+gDNAwiper) (Vazyme Biotech Co., Ltd, Nanjing, China) with RT-miR-specific primers using the stem-loop method. Briefly, 2 μL of 5 × gDNA wiper Mix, 1 μg of total RNA, and RNase-free double-distilled water were added to a 200 μL centrifuge tube to make 10 μL, mixed by pipetting, and reacted at 42 °C for 2 min after instantaneous centrifugation to remove genomic DNA; 2 μL of 10 × RT Mix, 2 μL of HiScript III Enzyme Mix, 0.2 μL of RT-miR-specific primers (10 μM), and 5.8 μL of RNase-free double-distilled water were continued in the centrifuge tube, mixed by pipetting, reacted at 37 °C for 15 min after instantaneous centrifugation, and reacted at 85 °C for 5 s. Quantification and purity testing of total RNA and miRNA were determined by NanoDrop 2000 spectrophotometer (Thermo Fisher Scientific, Inc.). qPCR experiments were performed according to ChamQ Universal SYBR qPCR Master Mix (Vazyme Biotech Co., Ltd, Nanjing, China). The system was as follows: 2 × Mix 10 μL, Primer-F (10 μM) 0.4 μL, Primer-R (10 μM) 0.4 μL, cDNA 1 μL, ddH_2O 8.2 μL. qPCR reaction conditions: pre-denaturation at 95 °C for 30 s; 40 cycles reaction at 95 °C for 10 s, 60 °C for 30 s; melting curve at 95 °C for 15 s, 60 °C for 60 s, 95 °C for 15 s. GAPDH and U6 were used as internal references, respectively [17,18], and the results were analyzed using the $2^{-\Delta\Delta Ct}$ method to normalize the relative expression of different factors, respectively [19]. All the primers applied in this study were listed in Table S1.

2.3. Oxygenation index (PaO_2/FiO_2)

Femoral arteries were isolated from mice, and 1 mL of femoral arterial blood was taken for immediate blood gas analysis to record PaO_2; According to the oxygen concentration fraction FiO_2 in the inhaled gas, the oxygenation index PaO_2/FiO_2 was calculated.

2.4. HE staining

Lung tissues were fixed in 4% paraformaldehyde overnight, dehydrated with graded ethanol and embedded in paraffin, sectioned at 4 μm, and stained with hematoxylin and eosin (HE). Pathological images were examined by light microscopy (ZEISS, Shanghai, China).

2.5. Pulmonary index

Lung weight (mg)/body weight (g) is the lung index. After the mice died, their total body weight was weighed, their lungs were measured for lung weight, and the lung index was calculated.

2.6. Lung water content

Measurement of lung water content: the wet/dry weight (W/D) ratio indicates the lung tissue water content. After the mice were sacrificed, their lungs were taken, the wet lungs were weighed, the wet lungs were dried at 60 °C for 7 days, and the dry lungs were weighed after drying.

2.7. NO content determination

Centrifuge the mouse blood to take the supernatant, add the samples and required reagents in turn according to the instructions for use of NO content detection kit (Solarbio, Beijing, China), Briefly, dilute the standard with distilled water to 0.2, 0.1, 0.05, 0.025, 0.0125, 0.00625 and 0.003125 μmol/mL standard solution by doubling; blank tube 120 μL of distilled water, standard tube 20 μL of distilled water + 100 μL of standard solution, test tube 100 μL of sample + 20 μL of Reagent I, all three vortex well, 37 °C water bath for 1 h; add 20 μL of Reagent II to each tube, vortex well, allow to stand at room temperature for 5 min, centrifuge at 3500 rpm for 10 min, transfer 100 μL of supernatant into a new tube; add 100 μL of chromogenic solution to 100 μL of supernatant in the new tube, vortex well. Allow to stand at room temperature for 10 min and measure the absorbance at 550 nm in a 96-well plate.

2.8. Enzyme-linked immunosorbent assay (Elisa)

The right main bronchus of the mice was ligated and the bronchoalveoli were lavaged with pre-chilled PBS, which was repeated three times, and the bronchoalveolar lavage fluid was collected. After the pulmonary microvascular endothelial cells were treated with LPS and miR-346 inhibitor, the supernatant was taken by centrifugation for future use. IL-1β, IL-6, and TNF-α protein contents in lung lavage fluid and cell supernatant were measured according to the instructions of Elisa kit (Solarbio, Beijing, China).

2.9. Cell culture and treatment

Human pulmonary microvascular endothelial cells (HPMECs) were purchased from Sunncell Biotech Co., Ltd. (China). These cells were cultured in DMEM medium (Dalian Meilun Biotech Co., Ltd., China) supplemented with 10% fetal bovine serum (FBS) and 100 U/mL penicillin and 100 μg/mL streptomycin and grown at 37 °C in a 5% CO_2 incubator. Cells were cultured to 80% confluency and used for experiments in this study. Trypsin (Dalian Meilun Biotech Co., Ltd., China) was used to passage cells.

According to previous studies [20,21], cells were treated with LPS (1 mg/L) or the same dose of saline for 24 h and then collected. Huzhou Hippo Biotechnology Co., Ltd. (China) created inhibitors of miR-346 (miR-346 inhibitor) and negative controls (nc inhibitor), small interfering RNA targeting BCL6 (si-BCL6) and negative controls (si-NC).

These inhibitors were transfected into HPMECs using Entranster™-R (Entrangreen Biosystem, Ltd., China) in strict accordance with the manufacturer's guidelines.

2.10. Cell counting kit-8 (CCK-8) assay

Cells were seeded into 96-well plates to a final volume of 100 μL and transfected with siRNA after attachment and cultured at 37 °C in a 5% CO_2 incubator. Add 10 μL CCK-8 solution into a 96-well plate, and incubate in an incubator for 1–4 h. Finally, the absorbance value at 450 nm was detected with a microplate reader.

2.11. Plate cloning

In the experiment, cells in exponential growth phase were digested with 0.25% trypsin to prepare single cells, seeded in six-well plates at the same cell number, gently rotated to disperse the cells evenly, and cultured in a 37 °C incubator with 5% CO_2 for 1–3 weeks. The culture was terminated when macroscopic clones appeared in the dishes. The culture medium was discarded, washed 1–2 times with PBS, fixed with 4% paraformaldehyde at room temperature for 10 min, and after discarding the fixative, 1 ml of 1% crystal violet staining solution was added for 10 min at room temperature and washed with PBS several times.

2.12. Bromodeoxyuridine labeling (BrdU)

Cells were seeded in a well plate and 100 μmol/L BrdU was added before stopping the culture and incubated for 4 h at 37 °C. They were fixed with precooled 4% paraformaldehyde for 10 min; incubated with 0.3% Triton-100 for 10 min; incubated with 2 mol/L HCl at 37 °C for 30 min; and incubated with 0.1 mol/L sodium borate for 10 min. Sheep serum was blocked at room temperature for 30 min; BrdU antibody was added for overnight incubation at 4 °C; fluorescent secondary antibody was incubated; and DAPI was added to stain nuclei. For fluorescence microscopy, the number of BrdU-positive cells and blue-stained nuclei was counted.

2.13. Scratch test

Pulmonary microvascular endothelial cell migration was measured by scratch assay. Transfected lung microvascular endothelial cells were seeded in well plates, and when the cells grew to 80% density, scratches were performed and pictures were taken at 0 h and 24 h under a 4-fold microscope to analyze the migration ability.

2.14. Apoptosis assay

Apoptosis and Necrosis Assay Kit (Beyotime Biotechnology, Shanghai, China) was detected by Hoechst 33342 and Propidium Iodide (PI) double staining. At the end of cell treatment, wash the cells with PBS for 1–2 times, add 5 μL Hoechst staining solution and 5 μL PI staining solution to each sample, mix well, and incubate at 4 °C for 30 min. They were washed once with PBS and observed for fluorescence under a fluorescence microscope.

2.15. Vector construction and dual-luciferase assay

BCL6 was screened as a potential target gene of miR-346 by TargetScan (TargetScanHuman 8.0) and miRDB (miRDB - MicroRNA Target Prediction Database) online software. The BCL6-Luc reporter was constructed by cloning the BCL6 promoter fragment into the PGL3 Luc vector. We entrusted Hippo Biotechnology Co., Ltd. (China) to synthesize miR-346 mimics. The BCL6-Luc eukaryotic expression vector was co-transfected with miR-346 mimics into HPMECs. After 24 h of culture, cells were collected. LUC activity was detected using the Dual-Luciferase Reporter Assay System (Promega, Madison, WI, USA).

2.16. Data analysis

All experiments were repeated three times. GraphPad Prism 5 software was used for data analysis, and the measurement results were expressed as mean ± standard deviation (mean ± SD). Data were analyzed for significance using the DPS 9.01 software Tukey algorithm. Differences by letter were significant at $P < 0.05$.

3. Results

3.1. miR-346 expression is increased in ARDS

To investigate the role of miR-346 in ARDS, we first performed sequence alignment of miR-346 in mice, and rats. The results showed that miR-346 was highly homologous in human, mouse and rat (Fig. 1A), so we stimulated mice with LPS to construct ARDS model. HE staining revealed severe lung injury after LPS stimulation (Fig. 1B), oxygenation index PaO_2/FiO_2 was significantly decreased (Fig. 1C), while lung water content, NO, inflammatory factors in lung tissue, inflammatory factors in bronchoalveolar lavage fluid, and apoptotic factors in lung tissue were increased (Fig. 1D–H), which indicated that the mouse ARDS model was successfully constructed. Afterwards, we examined the expression of miR-346 in ARDS lung tissues. RT-qPCR results showed that miR-346 expression was increased in LPS-induced ARDS lung tissues of mice (Fig. 1I), and miR-346 expression was negatively correlated with oxygenation index PaO_2/FiO_2 (Fig. 1J), all of which indicated that miR-346 may be involved in the ARDS process.

3.2. miR-346 can promote lung injury

To investigate the effect of miR-346 on lung tissue, we constructed a miR-346 inhibitor mouse lung injury model (Fig. 2A). Mice were sacrificed to retain lung tissue and sections were done for HE staining (Fig. 2B), which revealed that the degree of lung injury was relieved after inhibition of miR-346. Other parameters of lung injury after inhibition of miR-346, such as lung index, PaO_2/FiO_2, and lung water content, were also examined (Fig. 2C–E), and these results all showed that lung injury was alleviated after inhibition of miR-346. Afterwards, we also found that after inhibition of miR-346, the expression of proinflammatory factors such as IL-1β, TNF-α, and IL-6 in lung tissue was significantly reduced (Fig. 2F), NO content was significantly reduced (Fig. 2G), the expression of inflammatory factors in bronchoalveolar lavage fluid was reduced (Fig. 2H), and Bax expression in lung tissue was significantly reduced (Fig. 2I). The above results showed that miR-346 was able to promote lung injury.

3.3. miR-346 inhibits pulmonary microvascular endothelial cell function

From the above results, it can be seen that miR-346 has an effect on lung injury, and to clarify its function in lung injury, first we examined the expression of miR-346 in HPMECs and found that miR-346 expression was significantly increased in LPS-induced HPMECs (Fig. 3A), implying that it plays an important role in lung injury. Afterwards, we transfected HPMECs with miR-346 inhibitor (Fig. 3B). We detected their proliferation by CCK8, BrdU and plate cloning methods, and found that the cell proliferation ability was enhanced after inhibiting miR-346 (Fig. 3C–F); the migration function of miR-346 on HPMECs was examined by scratch assay, and it was found that the migration of HPMECs was enhanced after inhibiting miR-346 (Fig. 3G–H), and Hoechst/PI staining revealed that the apoptosis was alleviated after inhibiting miR-346 (Fig. 3I–J). RT-qPCR experiments revealed that IL-1β, IL-6, and TNF-α mRNA levels were significantly reduced when miR-346 expression was decreased in the cells (Fig. 3K), and the expression of chemokines CCL2 and adhesion factors I-CAM and V-CAM was significantly reduced

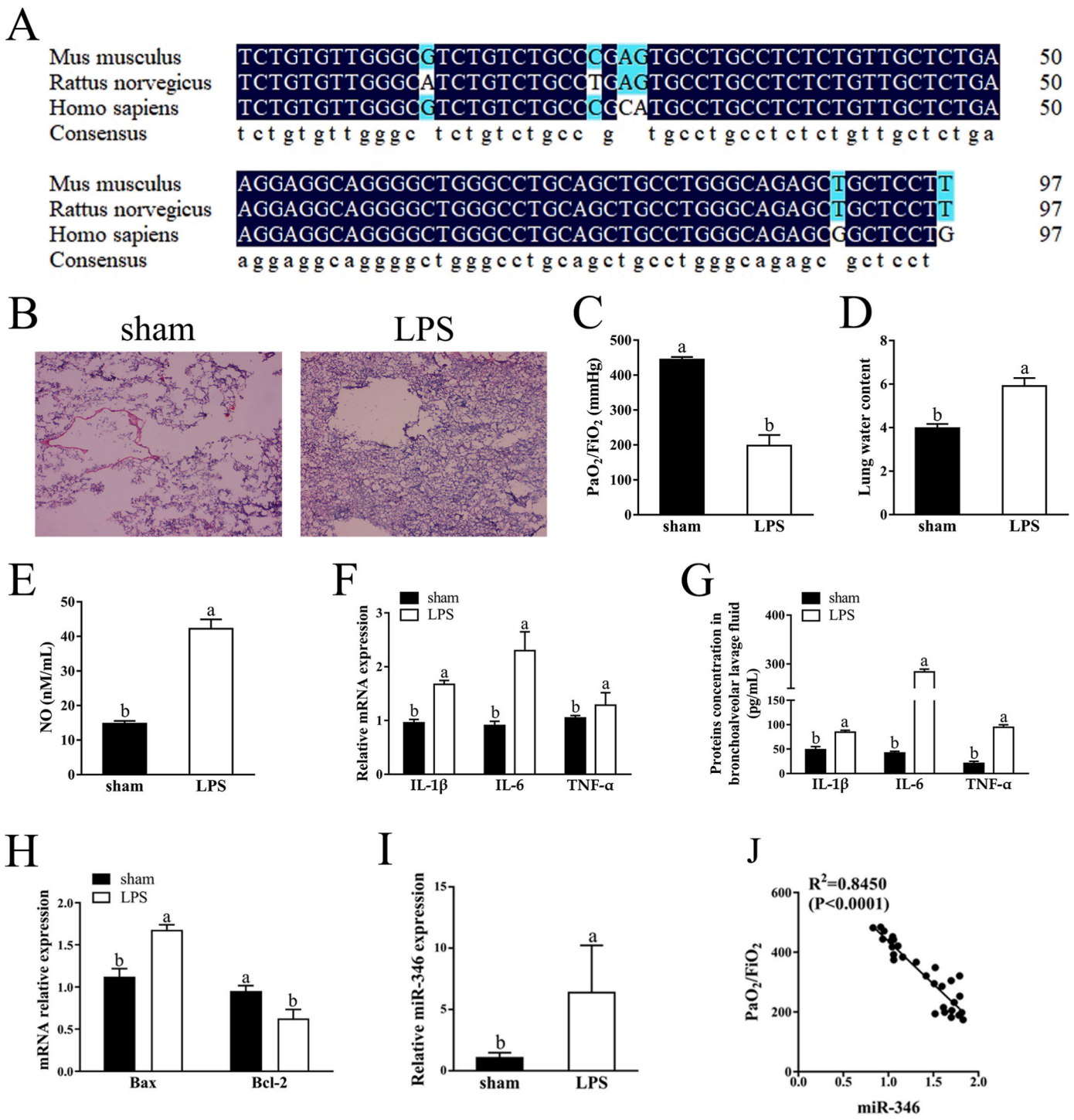

Fig. 1. miR-346 expression is increased in ARDS A. miR-346 sequence alignment of mouse, rat, and human; B. Increased lung tissue injury after LPS induction (n = 3); C. PaO_2/FiO_2 decreased after LPS induction (n = 3); D. Increased lung water content was induced by LPS (n = 3); E. NO content was significantly increased after LPS induction (n = 3); F. The mRNA levels of IL-1β, TNF-α, and IL-6 in lung tissue were significantly increased by LPS induction (n = 3); G. The contents of IL-1β, TNF-α, and IL-6 in the bronchoalveolar lavage fluid of mice were significantly increased after LPS induction (n = 3); H. Bax expression was increased in lung tissue after LPS induction, while Bcl-2 expression was significantly decreased (n = 3). I. miR-346 expression is increased in the lung tissue of ARDS mice (n = 3); J. miR-346 expression is inversely correlated with PaO_2/FiO_2 in mouse lung tissue (n = 29). The measurement results were expressed as mean ± standard deviation (mean ± SD). Differences by letter were significant at $P < 0.05$.

(Fig. 3L), demonstrating that miR-346 was able to promote lung inflammation. At the same time, CCL2, IL-1β, IL-6, and TNF-α protein levels were also significantly reduced in the cell supernatant (Fig. 3M), further indicating that miR-346 is proinflammatory. These results all indicate that miR-346 has an inhibitory effect on the biological activity of HPMECs and promotes lung injury.

3.4. BCL6 promotes the function of pulmonary microvascular endothelial cells

We predicted the possible target genes of miR-346 by TargetScan (TargetScanHuman 8.0) and miRDB (miRDB - MicroRNA Target Prediction Database) online software, and selected the common target

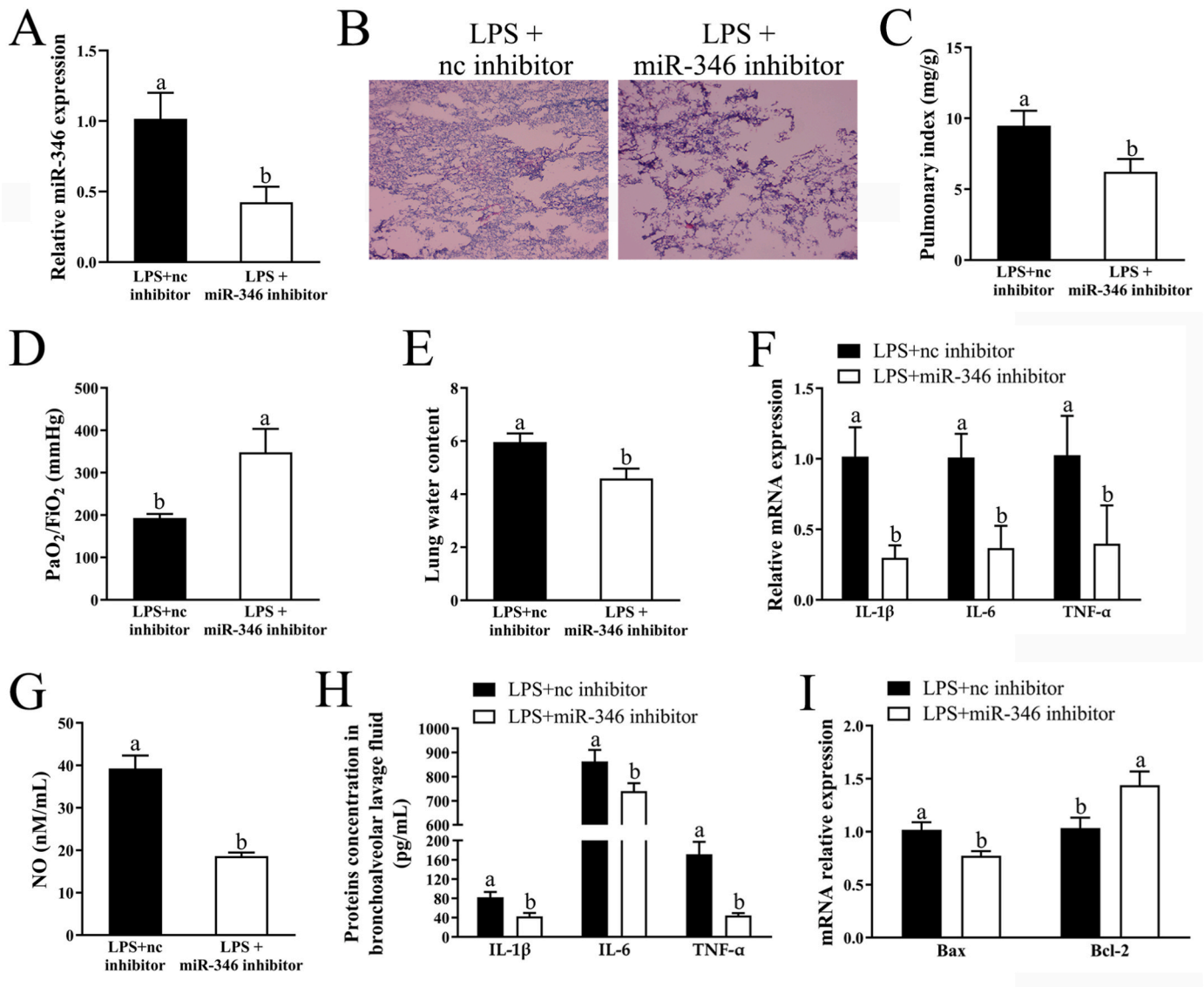

Fig. 2. miR-346 can promote lung injury

A. RT-qPCR verified that miR-346 expression was significantly reduced after *in vivo* inhibition of miR-346 (n = 3); B. HE staining showed reduced lung injury in mice that inhibited miR-346 (n = 3); C. Lung index was reduced after inhibition of miR-346 (n = 3); D. PaO_2/FiO_2 increased after decreased miR-346 expression (n = 3); E. Water content in lung tissue was decreased after inhibition of miR-346 (n = 3); F. mRNA expression levels of IL-1β, TNF-α, and IL-6 in lung tissue after inhibition of miR-346 (n = 3); G. NO content was significantly decreased after decreased miR-346 expression (n = 3); H. IL-1β, TNF-α, and IL-6 contents in the bronchoalveolar lavage fluid of mice were significantly reduced after inhibition of miR-346 (n = 3); I. Bax mRNA levels were decreased and Bcl-2 expression was significantly increased after decreased miR-346 expression (n = 3). The measurement results were expressed as mean ± standard deviation (mean ± SD). Differences by letter were significant at $P < 0.05$.

BCL6 with a higher score as the study object. After predicting the binding site of miR-346 to BCL6 using online software (Fig. 4A), the direct binding of miR-346 to BCL6 was verified by dual-luciferase assay (Fig. 4B).to further clarify whether miR-346 affects the function of HPMECs by regulating BCL6, we transfected pulmonary microvascular endothelial cell lines with miR-346 inhibitor and found that BCL6 expression was up-regulated (Fig. 4C–D). Subsequently, we inhibited the expression of BCL6 (Fig. 4E–F) while inhibiting miR-346 to see whether the function of miR-346 could be reversed. It was found that when inhibiting the expression of miR-346 and inhibiting BCL6, it inhibited both the proliferation (Fig. 4G–J) and migration ability (Fig. 4K-L) of HPMECs, and was able to promote the apoptosis of HPMECs (Fig. 4M – N), while the expression of inflammatory factors in the cells was increased after simultaneous inhibition of miR-346 and BCL6 (Fig. 4O). This indicates that BCL6 can promote the biological function of HPMECs, while miR-346 in the results 3 has an inhibitory effect on the biological activity of pulmonary vascular endothelial cells. This suggests that miR-346 is able to affect the biological function of lung endothelial cells by regulating the expression of BCL6.

3.5. *BCL6 relieves lung injury*

From the result 4, BCL6 promoted the biological function of HPMECs, and to further clarify the effect of BCL6 on lung tissue, a miR-346 inhibitor mouse lung injury model was constructed to detect a significant increase in the protein level of BCL6 in lung tissue (Fig. 5A–B). BCL6 was inhibited on the basis of lung injury in miR-346 inhibitor mice, and the mice were sacrificed to retain lung tissue and sections were done for HE staining, which revealed that the degree of lung injury increased after inhibition of BCL6 (Fig. 5C). Other parameters of lung injury after inhibition of BCL6, such as lung index, PaO_2/FiO_2, and lung water content, were also examined (Fig. 5D–F), and these

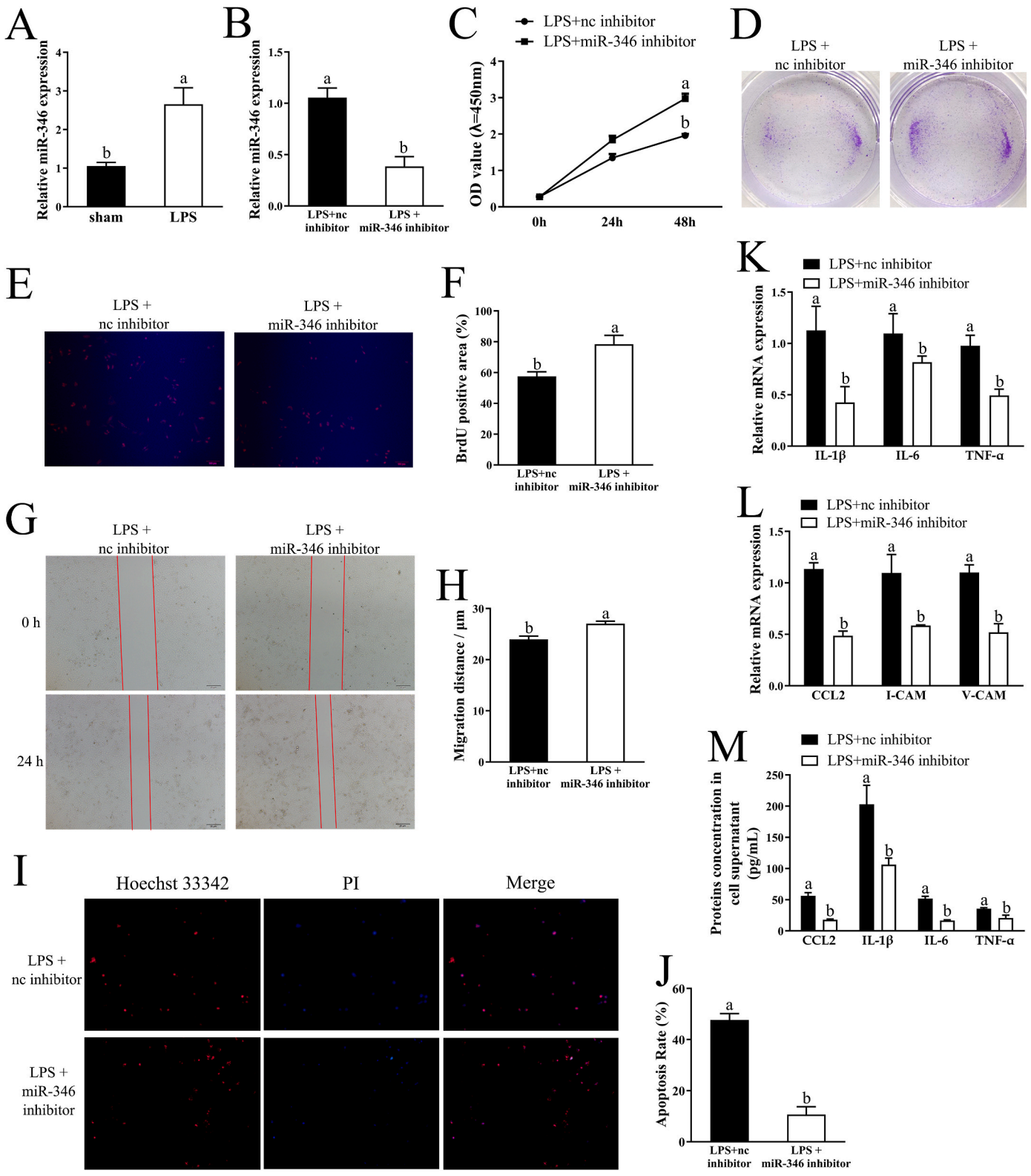

Fig. 3. miR-346 inhibits pulmonary microvascular endothelial cell function

A. miR-346 expression is increased in HPMECs after induction with LPS (n = 3); B. miR-346 expression was significantly reduced after inhibition of miR-346 (n = 3); C–F. CCK8, plate cloning and BrdU assay showed enhanced cell proliferation ability after reduced miR-346 expression (n = 3); G-H. Scratch assay were used to detect the enhanced migration ability of HPMECs after inhibition of miR-346 (n = 3); I-J. Hoechst/PI staining showed attenuated apoptosis after inhibition of miR-346 (n = 3); K. Inhibition of miR-346 in HPMECs could reduce inflammatory cytokines IL-1β, IL-6, and TNF-α expression (n = 3); L. The expression of chemokine CCL2 and adhesion factors I-CAM and V-CAM was significantly reduced in cells after inhibition of miR-346 (n = 3); M. CCL2, IL-1β, IL-6, and TNF-α contents in cell supernatants decreased with decreasing miR-346 expression (n = 3). The measurement results were expressed as mean ± standard deviation (mean ± SD). Differences by letter were significant at $P < 0.05$.

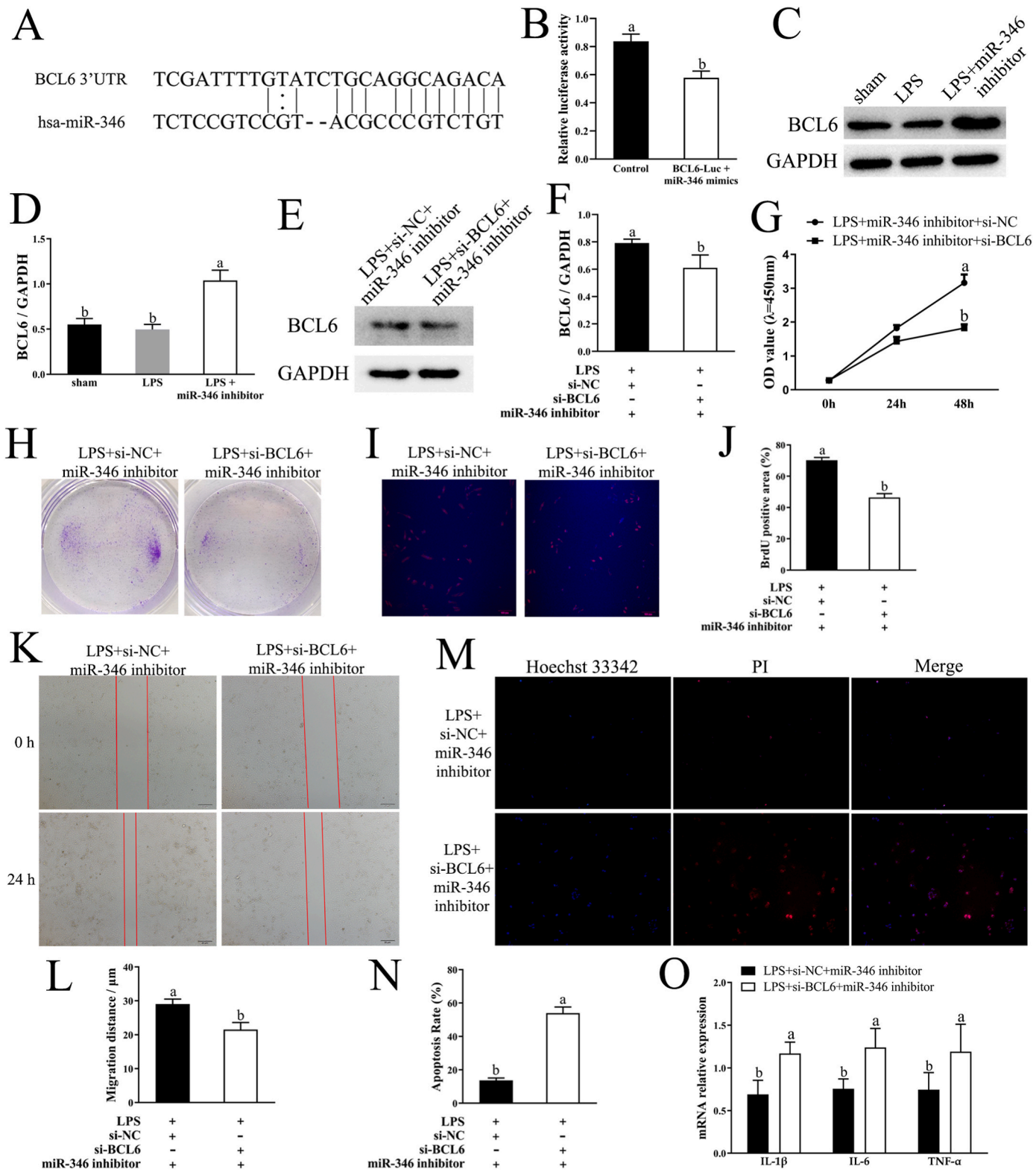

Fig. 4. Effect of BCL6 on pulmonary microvascular cell inflammation A. Predicted binding site of miR-346 to BCL6; B. Dual-luciferase assay to validate direct binding of miR-346 to BCL6 (n = 3); C-D. BCL6 expression was enhanced after inhibition of miR-346 (n = 3); E-F. BCL6 protein levels were significantly reduced after transfection with si-BCL6 (n = 3); G-J. CCK8, plate cloning and BrdU assay showed that the cell proliferation ability was attenuated after reduced BCL6 expression (n = 3); K-L. Scratch assay indicated that cell migration was attenuated after simultaneous inhibition of miR-346 and BCL6 (n = 3); M-N. Hoechst/PI experiments indicated enhanced apoptosis ability when inhibiting both miR-346 and BCL6 (n = 3); O. Simultaneous inhibition of miR-346 and BCL6 significantly increased the mRNA levels of IL-1β, IL-6, and TNF-α in the cells (n = 3). The measurement results were expressed as mean ± standard deviation (mean ± SD). Differences by letter were significant at $P < 0.05$.

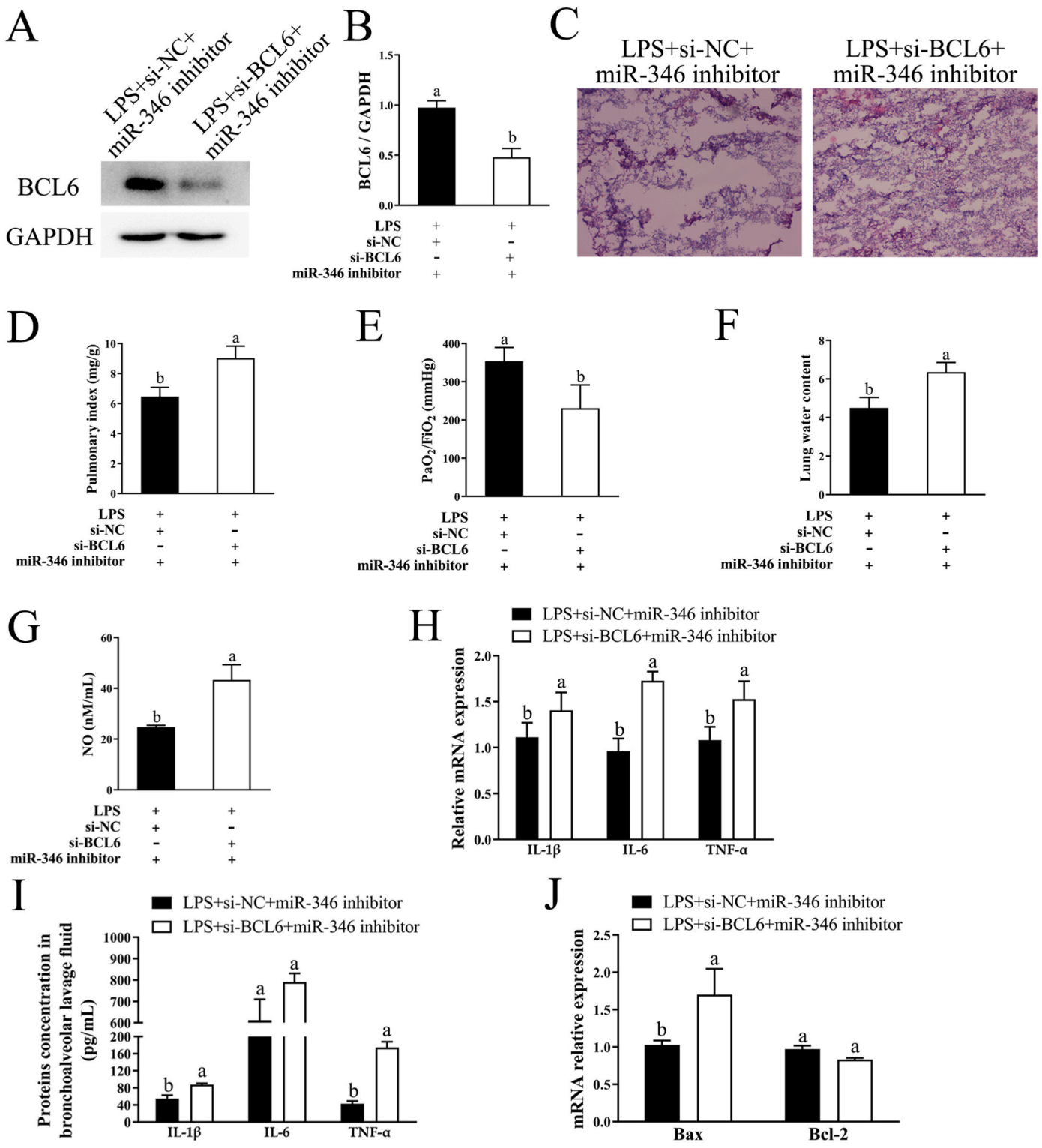

Fig. 5. BCL6 alleviates lung injury A-B. BCL6 expression was decreased in lung tissue after inhibition of BCL6 (n = 3); C. HE staining showed increased lung injury after inhibition of BCL6 (n = 3); D. Lung index was significantly increased after simultaneous inhibition of miR-346 and BCL6 (n = 3); E. PaO_2/FiO_2 decreased after inhibition of BCL6 (n = 3); F. Water content in lung tissue increased after decreased expression of miR-346 and BCL6 (n = 3); G. NO content was significantly increased after simultaneous inhibition of miR-346 and BCL6 (n = 3); H. mRNA levels of IL-1β, TNF-α, and IL-6 in lung tissue were increased after inhibition of miR-346 and BCL6 (n = 3); I. IL-1β, TNF-α, and IL-6 contents were significantly increased in the bronchoalveolar lavage fluid of mice after inhibition of miR-346 and BCL6 (n = 3); J. Bax mRNA levels were increased and Bcl-2 expression was significantly decreased in lung tissue after inhibition of BCL6. The measurement results were expressed as mean ± standard deviation (mean ± SD). Differences by letter were significant at $P < 0.05$.

results all showed aggravated lung injury after inhibition of BCL6. Afterwards, we also found that after inhibition of BCL6, NO content was significantly increased (Fig. 5G), the expression of proinflammatory factors such as IL-1β, TNF-α, and IL-6 in lung tissue was significantly increased (Fig. 5H), the content of inflammatory factors in bronchoalveolar lavage fluid was increased (Fig. 5I), Bax expression in lung tissue was significantly increased while Bcl2 and caspase3 were significantly decreased (Fig. 5J). The above results showed that BCL6 was able to alleviate lung injury. In summary, miR-346 is able to affect lung injury by regulating the expression of BCL6.

4. Discussion

In recent years, miRNAs have received increasing attention because of their key roles in the formation and development of various diseases. It has been shown that miRNAs are involved in the regulation of a variety of biological processes, such as cell proliferation, migration, and apoptosis, and that a variety of miRNAs have been identified in different cell types and disease settings. ARDS is a major cause of acute respiratory failure and is often accompanied by symptoms of multiple organ failure [22], resulting in increased patient distress, so it is necessary to study its pathogenesis. The generation of microRNAs is a highly regulated process with many influencing factors, including inflammatory responses such as ARDS. In recent years, studies on ARDS patients have found that miRNA expression is abnormal. CEES [23] exposure can also lead to differential expression of miRNAs in rat plasma [24]. It has been found that miR-346 expression is upregulated in rats, targeting multiple mRNAs [16]. In this study, we found that the expression of miR-346 was significantly up-regulated in lung tissue and LPS-stimulated HPMECs of ARDS patients, and after inhibition of miR-346, both cell proliferation and migration were enhanced, and apoptosis was attenuated, suggesting that miR-346 may be involved in ARDS by regulating the biological function of HPMECs.

The results of multiple studies showed that miRNAs are involved in ARDS, such as miR-21 [25], miR-155-5p [14], and miR-34a [13], miR-140-5p [24]. Studies have shown that miR-346 promotes HCC progression by inhibiting the expression of BRMS1 [26]; miR-346 can regulate EG-VEGF-induced trophoblast invasion by inhibiting the expression of MMP-2 and MMP-9 [27]; miR-346 is up-regulated in HCC cell lines, and its overexpression can promote the proliferation, migration and invasion of HCC cells [28]; miR-346 can reduce the expression of SMAD3/4 gene in the renal tissue of mice with diabetic nephropathy, thereby improving renal function [29]. The involvement of BCL6 in lung adenocarcinoma is negatively regulated by miR-339-5p [30]; loss of BCL6 in neutrophils attenuates lung inflammation [31]. However, in ARDS, the functions of miR-346 and BCL6 have not been reported. Many studies have shown that lipopolysaccharide (LPS) is an inducible proinflammatory factor [25], so in this study we constructed ARDS model mice through LPS induction to explore the mechanism of ARDS. Given that TNF-α and IL-6 act as proinflammatory factors [32,33], we examined the expression of TNF-α and IL-6 after LPS induction.

Pulmonary edema is an important link in the pathogenesis of ARDS. In this experiment, the degree of pulmonary edema was assessed by measuring the lung dry-wet weight ratio and lung index [34]. The results showed that inhibition of miR-346 could significantly attenuate the development of pulmonary edema in ARDS mice. NO can inhibit oxidative stress through a series of reactions, thereby protecting endothelial cells from apoptosis [35]. In this study, NO content was significantly increased after LPS induction, but decreased when miR-346 was inhibited, and apoptosis was attenuated after miR-346 inhibition. Inflammation is a major pathological event in ARDS [36], while miR-346 inhibits the progression of inflammation. HE staining showed that decreased miR-346 expression also attenuated the degree of pathological injury in lung tissue. BCL6 was predicted by targetscan and miRDB as a target of miR-346, BCL6 expression was increased when miR-346 was inhibited, and BCL6 could reverse the effect of miR-346 on ARDS.

The etiology of ARDS is complex and diverse. In this study, we confirmed the specific mechanism of action of miR-346 involved in the pathogenesis of ARDS through model construction and cellular level: to detect the changes of miR-346 expression levels in the lung tissue of ARDS mice, then combined with in vitro cellular experiments, to investigate whether miR-346 has a regulatory effect on BCL6, in order to explore the pathogenesis of ARDS and provide a new target and basis for clinical treatment. The results showed that the up-regulation of miR-346 in ARDS resulted in the decreased expression of BCL6 in lung endothelial cells, which in turn attenuated the proliferation and migration of HPMECs and increased the apoptotic effect of HPMECs, thereby decreasing the survival rate of lung endothelial cells, promoting apoptosis, producing inflammation, leading to lung injury, and then inducing ARDS. Targeted regulation of miR-346-BCL6 signaling pathway may become an effective approach for clinical treatment of ARDS. This study is important to further explore the molecular mechanism of lung injury and provides a new direction for clinical prevention and treatment of the occurrence of lung injury.

5. Conclusion

miR-346 inhibits the proliferation and migration of pulmonary microvascular endothelial cells by regulating BCL6 expression, which in turn promotes the apoptosis of pulmonary microvascular endothelial cells, leading to inflammation and inducing ARDS.

Credit author statement

JJ, All authors contributed to the study conception and design. Material preparation, data collection and analysis were performed by, The first draft of the manuscript was written by, all authors commented on previous versions of the manuscript. All authors read and approved the final manuscript, FG, All authors contributed to the study conception and design. Material preparation, data collection and analysis were performed by, all authors commented on previous versions of the manuscript. All authors read and approved the final manuscript, WL. All authors contributed to the study conception and design. Material preparation, data collection and analysis were performed by, all authors commented on previous versions of the manuscript. All authors read and approved the final manuscript, XS. All authors contributed to the study conception and design. Material preparation, data collection and analysis were performed by, all authors commented on previous versions of the manuscript. All authors read and approved the final manuscript

Funding

This work received no funding from any source.

Data availability statements

The datasets generated during and/or analyzed during the current study are available from the corresponding author on reasonable request.

Ethics approval

This study was performed in line with the principles of the Declaration of Helsinki and all animal experimental approved by the Animal Ethics Committee of Yuhuangding Hospital.

Declaration of competing interest

The authors declare that there is no conflict of interest regarding the publication of this paper.

Acknowledgements

No applicable.

Appendix A. Supplementary data

Supplementary data to this article can be found online at https://doi.org/10.1016/j.ncrna.2023.08.006.

References

[1] J.G. Laffey, M.A. Matthay, Fifty years of research in ARDS. Cell-Based therapy for acute respiratory distress syndrome. Biology and potential therapeutic value, Am. J. Respir. Crit. Care Med. 196 (3) (2017) 266–273, https://doi.org/10.1164/rccm.201701-0107CP.

[2] A.D.T. Force, V.M. Ranieri, G.D. Rubenfeld, B.T. Thompson, N.D. Ferguson, E. Caldwell, E. Fan, L. Camporota, A.S. Slutsky, Acute respiratory distress syndrome: the Berlin Definition, JAMA 307 (23) (2012) 2526–2533, https://doi.org/10.1001/jama.2012.5669.

[3] C. Guerin, J. Reignier, J.C. Richard, P. Beuret, A. Gacouin, T. Boulain, E. Mercier, M. Badet, A. Mercat, O. Baudin, M. Clavel, D. Chatellier, S. Jaber, S. Rosselli, J. Mancebo, M. Sirodot, G. Hilbert, C. Bengler, J. Richecoeur, M. Gainnier, F. Bayle, G. Bourdin, V. Leray, R. Girard, L. Baboi, L. Ayzac, P.S. Group, Prone positioning in severe acute respiratory distress syndrome, N. Engl. J. Med. 368 (23) (2013) 2159–2168, https://doi.org/10.1056/NEJMoa1214103.

[4] T.R. Craig, M.J. Duffy, M. Shyamsundar, C. McDowell, C.M. O'Kane, J.S. Elborn, D. F. McAuley, A randomized clinical trial of hydroxymethylglutaryl- coenzyme a reductase inhibition for acute lung injury (The HARP Study), Am. J. Respir. Crit. Care Med. 183 (5) (2011) 620–626, https://doi.org/10.1164/rccm.201003-0423OC.

[5] G.R. Bernard, A. Artigas, K.L. Brigham, J. Carlet, K. Falke, L. Hudson, M. Lamy, J. R. Legall, A. Morris, R. Spragg, t.C. Committee, The American-European Consensus Conference on ARDS. Definitions, mechanisms, relevant outcomes, and clinical trial coordination, Am. J. Respir. Crit. Care Med. 149 (1994) 818–824.

[6] G. Bellani, J.G. Laffey, T. Pham, E. Fan, L. Brochard, A. Esteban, L. Gattinoni, F. van Haren, A. Larsson, D.F. McAuley, M. Ranieri, G. Rubenfeld, B.T. Thompson, H. Wrigge, A.S. Slutsky, A. Pesenti, L.S. Investigators, E.T. Group, Epidemiology, patterns of care, and mortality for patients with acute respiratory distress syndrome in intensive care units in 50 countries, JAMA 315 (8) (2016) 788–800, https://doi.org/10.1001/jama.2016.0291.

[7] Y. Abadie, F. Bregeon, L. Papazian, F. Lange, B. Chailley-Heu, P. Thomas, P. Duvaldestin, S. Adnot, B. Maitre, C. Delclaux, Decreased VEGF concentration in lung tissue and vascular injury during ARDS, Eur. Respir. J. 25 (1) (2005) 139–146, https://doi.org/10.1183/09031936.04.00065504.

[8] L. Biancone, S. Bruno, M.C. Deregibus, C. Tetta, G. Camussi, Therapeutic potential of mesenchymal stem cell-derived microvesicles, Nephrol. Dial. Transplant. 27 (8) (2012) 3037–3042, https://doi.org/10.1093/ndt/gfs168.

[9] H. Menden, S. Welak, S. Cossette, R. Ramchandran, V. Sampath, Lipopolysaccharide (LPS)-mediated angiopoietin-2-dependent autocrine angiogenesis is regulated by NADPH oxidase 2 (Nox2) in human pulmonary microvascular endothelial cells, J. Biol. Chem. 290 (9) (2015) 5449–5461, https://doi.org/10.1074/jbc.M114.600692.

[10] G. Song, R. Wang, J. Guo, X. Liu, F. Wang, Y. Qi, H. Wan, M. Liu, X. Li, H. Tang, miR-346 and miR-138 competitively regulate hTERT in GRSF1- and AGO2-dependent manners, respectively, Sci. Rep. 5 (2015), 15793, https://doi.org/10.1038/srep15793.

[11] Q. Wang, J. Cai, X.H. Cai, L. Chen, miR-346 regulates osteogenic differentiation of human bone marrow-derived mesenchymal stem cells by targeting the Wnt/beta-catenin pathway, PLoS One 8 (9) (2013), e72266, https://doi.org/10.1371/journal.pone.0072266.

[12] X. Lv, P. Lu, Y. Hu, T. Xu, miR-346 inhibited apoptosis against myocardial ischemia-reperfusion injury via targeting Bax in rats, Drug Des. Dev. Ther. 14 (2020) 895–905, https://doi.org/10.2147/DDDT.S245193.

[13] D. Shah, P. Das, M.A. Alam, N. Mahajan, F. Romero, M. Shahid, H. Singh, V. Bhandari, MicroRNA-34a promotes endothelial dysfunction and mitochondrial-mediated apoptosis in murine models of acute lung injury, Am. J. Respir. Cell Mol. Biol. 60 (4) (2019) 465–477, https://doi.org/10.1165/rcmb.2018-0194OC.

[14] J. Jiang, Z. Song, L. Zhang, miR-155-5p promotes progression of acute respiratory distress syndrome by inhibiting differentiation of bone marrow mesenchymal stem cells to alveolar type II epithelial cells, Med. Sci. Mon. Int. Med. J. Exp. Clin. Res. 24 (2018) 4330–4338, https://doi.org/10.12659/MSM.910316.

[15] L. Liu, Z. Yu, Q. Ma, J. Yu, Z. Gong, G. Deng, X. Wu, LncRNA NR_003508 suppresses Mycobacterium tuberculosis-induced programmed necrosis via sponging miR-346-3p to regulate RIPK1, Int. J. Mol. Sci. 24 (9) (2023), https://doi.org/10.3390/ijms24098016.

[16] C. Huang, X. Xiao, N.R. Chintagari, M. Breshears, Y. Wang, L. Liu, MicroRNA and mRNA expression profiling in rat acute respiratory distress syndrome, BMC Med. Genom. 7 (46) (2014).

[17] K. Li, Z. Huang, S. Tian, Y. Chen, Y. Yuan, J. Yuan, X. Zou, F. Zhou, MicroRNA-877-5p alleviates ARDS via enhancing PI3K/Akt path by targeting CDKN1B both in vivo and in vitro, Int. Immunopharm. 95 (2021), 107530, https://doi.org/10.1016/j.intimp.2021.107530.

[18] F. Xu, F. Zhou, Inhibition of microRNA-92a ameliorates lipopolysaccharide-induced endothelial barrier dysfunction by targeting ITGA5 through the PI3K/Akt signaling pathway in human pulmonary microvascular endothelial cells, Int. Immunopharm. 78 (2020), 106060, https://doi.org/10.1016/j.intimp.2019.106060.

[19] K.J. Livak, T.D. Schmittgen, Analysis of relative gene expression data using real-time quantitative PCR and the 2(-Delta Delta C(T)) Method, Methods 25 (4) (2001) 402–408, https://doi.org/10.1006/meth.2001.1262.

[20] M.-Y. Yao, W.-H. Zhang, W.-T. Ma, Q.-H. Liu, L.-H. Xing, G.-F. Zhao, Long non-coding RNA MALAT1 exacerbates acute respiratory distress syndrome by upregulating ICAM-1 expression via microRNA-150-5p downregulation, Aging (Albany NY) 12 (8) (2020) 6570–6585, https://doi.org/10.18632/aging.102953.

[21] Z. Fu, Z. Zhang, X. Wu, J. Zhang, Hydrogen-rich saline inhibits lipopolysaccharide-induced acute lung injury and endothelial dysfunction by regulating autophagy through mTOR/TFEB signaling pathway, BioMed Res. Int. 2020 (2020), 9121894, https://doi.org/10.1155/2020/9121894.

[22] M.A. Matthay, L.B. Ware, G.A. Zimmerman, The acute respiratory distress syndrome, J. Clin. Invest. 122 (8) (2012) 2731–2740, https://doi.org/10.1172/JCI60331.

[23] N. Mariappan, M. Husain, I. Zafar, V. Singh, K.G. Smithson, D.R. Crowe, J.F. Pittet, S. Ahmad, A. Ahmad, Extracellular nucleic acid scavenging rescues rats from sulfur mustard analog-induced lung injury and mortality, Arch. Toxicol. 94 (4) (2020) 1321–1334, https://doi.org/10.1007/s00204-020-02699-1.

[24] T. Rana, A. Ahmad, I. Zafar, N. Mariappan, D.S. Chandrashekar, T. Hamid, M. Husain, S. Varambally, S. Ahmad, A. Ahmad, MicroRNA-mediated inflammation and coagulation effects in rats exposed to an inhaled analog of sulfur mustard, Ann. N. Y. Acad. Sci. 1479 (1) (2020) 148–158, https://doi.org/10.1111/nyas.14416.

[25] W.D. Zhu, J. Xu, M. Zhang, T.M. Zhu, Y.H. Zhang, K. Sun, MicroRNA-21 inhibits lipopolysaccharide-induced acute lung injury by targeting nuclear factor-kappaB, Exp. Ther. Med. 16 (6) (2018) 4616–4622, https://doi.org/10.3892/etm.2018.6789.

[26] Z. Guo, J. Li, J. Sun, L. Sun, Y. Zhou, Z. Yu, miR-346 promotes HCC progression by suppressing breast cancer metastasis suppressor 1 expression, Oncol. Res. 26 (7) (2018) 1073–1081, https://doi.org/10.3727/096504017X15145088802439.

[27] M.T. Su, P.Y. Tsai, H.L. Tsai, Y.C. Chen, P.L. Kuo, miR-346 and miR-582-3p-regulated EG-VEGF expression and trophoblast invasion via matrix metalloproteinases 2 and 9, Biofactors 43 (2) (2017) 210–219, https://doi.org/10.1002/biof.1325.

[28] Q. Yu, X. Yang, W. Duan, C. Li, Y. Luo, S. Lu, miRNA-346 promotes proliferation, migration and invasion in liver cancer, Oncol. Lett. 14 (3) (2017) 3255–3260, https://doi.org/10.3892/ol.2017.6561.

[29] Y. Zhang, H.Q. Xiao, Y. Wang, Z.S. Yang, L.J. Dai, Y.C. Xu, Differential expression and therapeutic efficacy of microRNA-346 in diabetic nephropathy mice, Exp. Ther. Med. 10 (1) (2015) 106–112, https://doi.org/10.3892/etm.2015.2468.

[30] P. Li, H. Liu, Y. Li, Y. Wang, L. Zhao, H. Wang, miR-339-5p inhibits lung adenocarcinoma invasion and migration by directly targeting BCL6, Oncol. Lett. 16 (5) (2018) 5785–5790, https://doi.org/10.3892/ol.2018.9376.

[31] B. Zhu, R. Zhang, C. Li, L. Jiang, M. Xiang, Z. Ye, H. Kita, A.M. Melnick, A.L. Dent, J. Sun, BCL6 modulates tissue neutrophil survival and exacerbates pulmonary inflammation following influenza virus infection, Proc. Natl. Acad. Sci. U. S. A. 116 (24) (2019) 11888–11893, https://doi.org/10.1073/pnas.1902310116.

[32] G. Malleo, E. Mazzon, A.K. Siriwardena, S. Cuzzocrea, TNF-alpha as a therapeutic target in acute pancreatitis–lessons from experimental models, Sci. World J. 7 (2007) 431–448, https://doi.org/10.1100/tsw.2007.98.

[33] T. Tanaka, M. Narazaki, T. Kishimoto, IL-6 in inflammation, immunity, and disease, Cold Spring Harbor Perspect. Biol. 6 (10) (2014) a016295, https://doi.org/10.1101/cshperspect.a016295.

[34] Y. Zeng, H. Zhao, T. Zhang, C. Zhang, Y. He, L. Du, F. Zuo, W. Wang, Lung-protective effect of Punicalagin on LPS-induced acute lung injury in mice, Biosci. Rep. 42 (1) (2022), https://doi.org/10.1042/BSR20212196.

[35] H. Peng, S. Zhang, Z. Zhang, X. Wang, X. Tian, L. Zhang, J. Du, Y. Huang, H. Jin, Nitric oxide inhibits endothelial cell apoptosis by inhibiting cysteine-dependent SOD1 monomerization, FEBS Open Bio 12 (2) (2022) 538–548, https://doi.org/10.1002/2211-5463.13362.

[36] G. Liu, Q. Zheng, K. Pan, X. Xu, Protective effect of Chrysanthemum morifolium Ramat. ethanol extract on lipopolysaccharide induced acute lung injury in mice, BMC Complement Med Ther 20 (1) (2020) 235, https://doi.org/10.1186/s12906-020-03017-z.